A key mammalian cholesterol synthesis enzyme, squalene monooxygenase, is allosterically stabilized by its substrate

Hiromasa Yoshioka[a], Hudson W. Coates[b], Ngee Kiat Chua[b], Yuichi Hashimoto[a], Andrew J. Brown[b,1], and Kenji Ohgane[a,c,1]

[a]Institute for Quantitative Biosciences, The University of Tokyo, 113-0032 Tokyo, Japan; [b]School of Biotechnology and Biomolecular Sciences, University of New South Wales, Sydney, NSW 2052, Australia; and [c]Synthetic Organic Chemistry Laboratory, RIKEN, 351-0198 Saitama, Japan

Edited by Brenda A. Schulman, Max Planck Institute of Biochemistry, Martinsried, Germany, and approved February 18, 2020 (received for review September 20, 2019)

Cholesterol biosynthesis is a high-cost process and, therefore, tightly regulated by both transcriptional and posttranslational negative feedback mechanisms in response to the level of cellular cholesterol. Squalene monooxygenase (SM, also known as squalene epoxidase or SQLE) is a rate-limiting enzyme in the cholesterol biosynthetic pathway and catalyzes epoxidation of squalene. The stability of SM is negatively regulated by cholesterol via its N-terminal regulatory domain (SM-N100). In this study, using a SM-luciferase fusion reporter cell line, we performed a chemical genetics screen that identified inhibitors of SM itself as up-regulators of SM. This effect was mediated through the SM-N100 region, competed with cholesterol-accelerated degradation, and required the E3 ubiquitin ligase MARCH6. However, up-regulation was not observed with statins, well-established cholesterol biosynthesis inhibitors, and this pointed to the presence of another mechanism other than reduced cholesterol synthesis. Further analyses revealed that squalene accumulation upon treatment with the SM inhibitor was responsible for the up-regulatory effect. Using photoaffinity labeling, we demonstrated that squalene directly bound to the N100 region, thereby reducing interaction with and ubiquitination by MARCH6. Our findings suggest that SM senses squalene via its N100 domain to increase its metabolic capacity, highlighting squalene as a feedforward factor for the cholesterol biosynthetic pathway.

squalene | squalene monooxygenase | chemical genetics | cholesterol homeostasis

Cholesterol is essential as a component of cellular membranes and precursor for physiologically important steroids, including oxysterols, steroid hormones, and bile acids, but cholesterol can also be toxic in excess. Therefore, cholesterol homeostasis is tightly regulated by intricate networks of feedback loops at both transcriptional and posttranslational levels. Transcriptionally, a large number of genes involved in cholesterol biosynthesis or cholesterol uptake are controlled by the master transcriptional regulators, sterol-regulatory element binding proteins (SREBPs), in a sterol-responsive manner (1). In addition to this relatively slow feedback mechanism, cells have developed posttranslational mechanisms that act on a shorter time scale, in which the degradation of several cholesterol biosynthetic enzymes is accelerated in response to higher levels of cholesterol and/or oxysterols (2–6).

Squalene monooxygenase (SM, also known as squalene epoxidase or SQLE; EC:1.14.14.17) is a second rate-limiting enzyme in the cholesterol biosynthetic pathway and catalyzes epoxidation of squalene downstream of the first rate-limiting enzyme, 3-hydroxy-3-methylglutaryl-CoA reductase. Recent studies have revealed that SM is subjected to negative feedback regulation via accelerated degradation under cholesterol-rich conditions. SM senses excess cholesterol in the endoplasmic reticulum (ER) membrane through its N-terminal 100-residue regulatory region (SM-N100), and alters its own stability depending on the cholesterol concentration (5, 7, 8). Membrane-associated ring-CH type finger 6 (MARCH6) is the cognate E3 ligase for SM (9, 10), catalyzing its ubiquitination in the N100 region (11).

Despite its importance in cholesterol-accelerated degradation, the structure and function of the SM-N100 region has not been fully resolved. Thus far, biochemical analyses have revealed the presence of a reentrant loop anchoring SM to the ER membrane and an amphipathic helix required for cholesterol-accelerated degradation (7, 8), while X-ray crystallography has revealed the architecture of the catalytic domain of SM (12). However, the highly hydrophobic and disordered nature of the N100 region has hampered purification and structural analysis of this region or full-length SM (12, 13). To fully understand how SM-N100 functions and how SM proteostasis is regulated, different multidisciplinary approaches may assist.

In the present study, we used a chemical genetics approach to identify a regulatory factor of SM proteostasis. Screening of a library of bioactive compounds identified inhibitors of human SM itself as having a stabilizing effect on SM. Further analyses revealed that squalene, a cholesterol synthesis intermediate and SM substrate that accumulates upon SM inhibition, was responsible

Significance

Cholesterol is an essential component of cell membranes and a precursor for steroid hormones and bile acids. Squalene monooxygenase (SM) is a rate-limiting enzyme in the cholesterol biosynthetic pathway and has been demonstrated to be post-translationally regulated via a negative feedback mechanism that involves cholesterol-mediated degradation. Here, we revealed another regulatory mechanism for this enzyme through a chemical genetics screen. SM is stabilized by its substrate, squalene, via direct binding of squalene to its noncatalytic, N-terminal regulatory domain. Our findings suggest that squalene is not just an inert hydrocarbon in cholesterol synthesis but a more active feedforward regulator of the pathway and offers a renewed opportunity to modulate SM activity via allosteric modulation of its stability.

Author contributions: H.Y., H.W.C., N.K.C., Y.H., A.J.B., and K.O. designed research; H.Y., H.W.C., N.K.C., and K.O. performed research; H.Y., H.W.C., N.K.C., A.J.B., and K.O. analyzed data; and H.Y., H.W.C., N.K.C., Y.H., A.J.B., and K.O. wrote the paper.

The authors declare no competing interest.

This article is a PNAS Direct Submission.

Data deposition: Screening data have been deposited to Mendeley Data (http://doi.org/10.17632/53dxyt4rnd.1).

See online for related content such as Commentaries.

[1]To whom correspondence may be addressed. Email: ohgane@iam.u-tokyo.ac.jp or aj.brown@unsw.edu.au.

This article contains supporting information online at https://www.pnas.org/lookup/suppl/doi:10.1073/pnas.1915923117/-/DCSupplemental.

First published March 13, 2020.

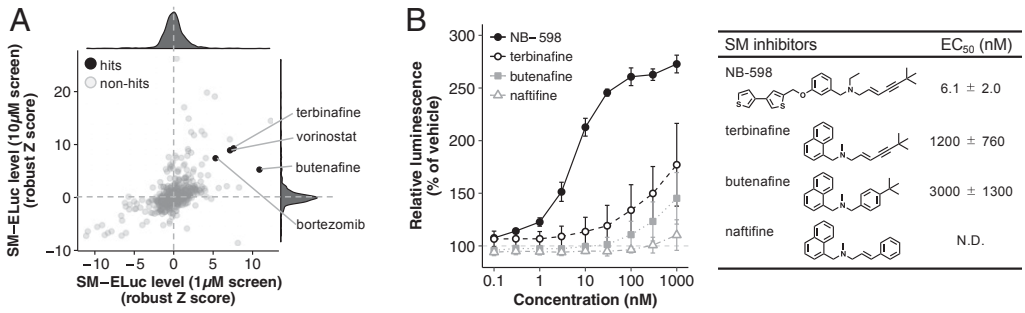

Fig. 1. A chemical screen identifies SM inhibitors as SM stabilizers. (*A*) HEK293 cells stably expressing SM-ELuc were treated with 1 μM or 10 μM test compounds for 16 h, and expression levels were quantified by luciferase assay. Hit compounds were those with a reproducible robust Z score of >5. (*B*) HEK293 cells stably expressing SM-ELuc were treated with the indicated concentrations of SM inhibitors for 16 h, and expression levels were quantified by luciferase assay (mean ± SD; $n = 3$ independent experiments). EC_{50} values are mean ± SD ($n = 3$ independent experiments). N.D., not determined.

for the stabilization, and the effect was mediated through the N100 region. Analyses using photoaffinity labeling demonstrated that squalene directly bound to the SM-N100 region in a specific manner, supporting a model in which squalene binding reduces interaction with MARCH6 and subsequent degradation. These findings indicate that SM senses squalene abundance via its N-terminal regulatory domain to increase the metabolic capacity at this step. Squalene, previously considered to be a relatively inert intermediate in cholesterol biosynthesis, may therefore have a more active role in regulating cholesterol synthesis as a key factor in a local feedforward mechanism.

Results

A Chemical Screen Identifies SM Inhibitors as SM Stabilizers. To understand how SM stability is regulated, we performed chemical genetic screening of 768 Food and Drug Administration (FDA)-approved drugs of known bioactivities using a luciferase-based assay monitoring SM stability. We stably transfected HEK293 cells with a plasmid encoding SM fused to emerald luciferase (SM-ELuc) (14, 15) under the control of a constitutive CMV promoter. This cell line allows sensitive monitoring of SM-ELuc expression by its luciferase activity in a high-throughput manner. From a screen of the library at 1 and 10 μM concentrations, we identified four potential hit compounds that gave a reproducible up-regulatory effect, including in follow-up assays using freshly purchased compounds (Fig. 1*A*). The four hits included two inhibitors of fungal SM, terbinafine and butenafine, the proteasome inhibitor bortezomib, and the histone deacetylase (HDAC) inhibitor vorinostat. Considering that SM turnover is primarily mediated through the proteasome-dependent ER-associated degradation (ERAD) pathway, we excluded bortezomib from later analyses as an obvious hit. We also excluded vorinostat as HDAC inhibitors can affect the activity of CMV promoters (16) and, therefore, could confound SM-ELuc reporter results, in addition to affecting global cellular proteostasis capacity, which would likely influence SM stability (17, 18).

Focusing on the SM inhibitors terbinafine and butenafine, we next examined their dose-dependent up-regulatory effect. Naftifine, another fungal SM inhibitor, was also tested. As fungal SM inhibitors tend to be relatively weak inhibitors of the human enzyme, we further tested the dose-dependent effects of NB-598, which has been developed as a highly potent inhibitor of human SM with in vitro inhibitory potency in the low nanomolar range (19). Each of the tested SM inhibitors up-regulated SM, and more potent inhibitors against human SM (20) stabilized SM more potently (EC_{50} for NB-598, 6.1 nM), suggesting that the observed up-regulation was likely mediated through the on-target inhibition of human SM (Fig. 1*B*).

NB-598 Up-Regulates SM Independent of the C-Terminal Catalytic Domain. The cholesterol-accelerated degradation of SM is mediated through the N-terminal regulatory domain, which consists of the first 100 residues (SM-N100). When SM-N100 is fused with other proteins, it confers susceptibility to cholesterol-accelerated degradation (5), indicating that this domain is a cholesterol-dependent degron (Fig. 2*A*). To determine if the up-regulatory effect by NB-598 is also mediated through this domain, we prepared two deletion mutant constructs of SM-ELuc, SM-N100-ELuc

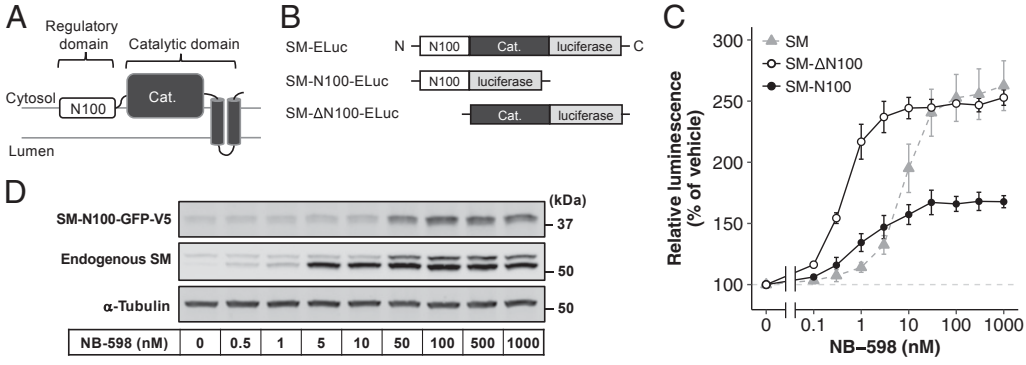

Fig. 2. The N-terminal regulatory domain of SM is sufficient for NB-598–mediated up-regulation. (*A*) Schematic representation of predicted SM topology. (*B*) Schematic representation of SM-ELuc deletion constructs. (*C*) HEK293 cells stably expressing SM-ELuc, SM-N100-ELuc, or SM-ΔN100-ELuc were treated with the indicated concentrations of NB-598 for 16 h, and expression levels were quantified by luciferase assay (mean ± SD; $n = 3$ independent experiments). (*D*) HEK293 cells stably expressing SM-N100-GFP-V5 were treated with the indicated concentrations of NB-598 for 16 h, and protein levels were determined by immunoblotting. For quantification, see *SI Appendix*, Fig. S1.

and SM-ΔN100-ELuc, and examined their behavior in the presence of varying concentrations of NB-598 (Fig. 2*B*). NB-598, which tightly binds to the active site of SM (12), up-regulated SM-ΔN100-ELuc with an EC_{50} of 0.44 nM (Fig. 2*C*). This observation is consistent with the fact that stabilization of the SM catalytic domain by NB-598 has been observed using in vitro thermal shift assays (12), and with the previously reported stabilization of receptors or enzymes upon binding of their ligands in living cells (21–24). Interestingly, NB-598 also up-regulated the SM-N100 regulatory domain in two different cell lines stably expressing SM-N100-ELuc (EC_{50} 1.3 nM) or SM-N100-GFP-V5 (EC_{50} 18 nM) constructs (Fig. 2 *C* and *D* and *SI Appendix*, Fig. S1). Stabilization of endogenous SM also occurred (Fig. 2*D*), confirming the relevance of the effect to the native enzyme. While detecting endogenous SM, we observed a second, lower-molecular weight band that was derived from SM (*SI Appendix*, Fig. S2) and more sensitive to NB-598 than the full-length protein (Fig. 2*D*). This truncated protein likely lacks the N100 domain, as the antibody used for detection was targeted against the SM catalytic domain and the shift in molecular weight was consistent with the loss of this fragment. Therefore, its stronger stabilization by NB-598 is consistent with that of SM-ΔN100-ELuc, perhaps due to the inherent stability conferred by the absence of the N100 degron. Together, our data indicated that in addition to direct binding and stabilization of the catalytic domain by NB-598, the SM-N100 region also mediated the stabilizing effects of the inhibitor.

NB-598–Mediated Stabilization Is Dependent on the Availability of Cholesterol Biosynthetic Intermediates. As SM-N100 is a cholesterol-responsive region, its stabilization by NB-598 highlights a possible regulatory role. To investigate this further, we tested the effects of NB-598 in medium containing lipoprotein-deficient serum (LPDS). Lacking cholesterol, LPDS prevents the uptake of cholesterol from the extracellular environment, inducing cholesterol depletion and activation of the SREBP pathway. This leads to up-regulation of cholesterogenic genes and increased flux through cholesterol synthesis. In LPDS, stabilization of SM-N100 and endogenous SM by NB-598 was greater than in medium containing normal, full serum (Fig. 3*A*). However, blocking cholesterol synthesis with the statin compactin prevented NB-598 from stabilizing these proteins in LPDS. This indicated that activity of the cholesterol synthesis pathway is required for the stabilizing effects of NB-598.

Next, we observed that pretreatment with NB-598 blunted the cholesterol-mediated degradation of SM-N100 and endogenous SM (Fig. 3*B*). This suggested that the mechanism of NB-598–mediated stabilization competes with the effects of cholesterol, perhaps by relying on similar effectors.

Stabilization of SM-N100 Is Mediated by Squalene Accumulation. As an active cholesterol synthesis pathway is required for the stabilizing effects of NB-598, we inhibited a number of steps in the pathway and measured SM-N100-ELuc stability (Fig. 4*A*). Only NB-598 significantly stabilized SM-N100-ELuc (Fig. 4*B*), implicating the intermediate upstream of SM, squalene, in this effect.

While levels of squalene were near the lower limits of detection in vehicle-treated cells (~200 pg of squalene per μg of cellular protein), NB-598 treatment induced a dramatic and dose-dependent 30-fold accumulation, consistent with inhibition of SM activity (Fig. 4*C* and *SI Appendix*, Fig. S3, EC_{50} for squalene accumulation 13 nM). Significantly, we noted that SM-N100-ELuc luminescence increased in a nonlinear, saturable manner in response to the accumulation of squalene (Fig. 4*D*). This implied that SM-N100-ELuc stability increases even with small increases in squalene levels. These data showed that accumulated squalene is likely to be responsible for the stabilization of SM-N100 by NB-598.

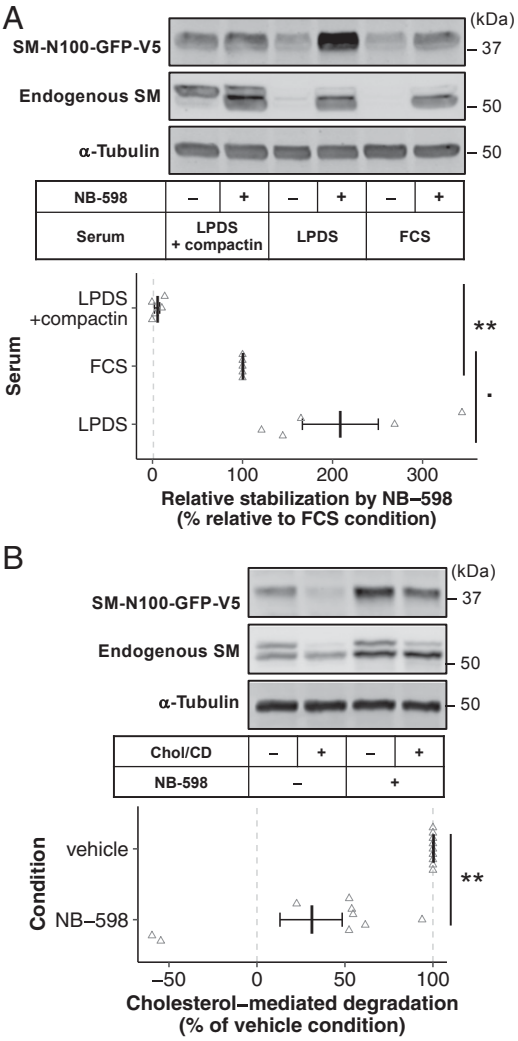

Fig. 3. NB-598–mediated stabilization of SM-N100 depends on the availability of cholesterol biosynthetic intermediates. (*A*) HEK293 cells stably expressing SM-N100-GFP-V5 were conditioned in medium containing fetal calf serum (FCS), LPDS, or LPDS plus 5 μM compactin and 50 μM mevalonate for 8 h, then treated in conditioning medium with or without 1 μM NB-598 for 16 h. Graph shows densitometric representation of immunoblot of SM-N100-GFP-V5 levels. Data were normalized to NB-598–mediated stabilization in the FCS condition, which was set to 100%. Black lines and error bars denote mean ± SEM, and gray open triangles denote raw data points from each of $n = 5$ independent experiments (•$P < 0.1$, *$P < 0.05$, **$P < 0.01$, two-sided paired *t* test versus FCS with the Benjamini-Hochberg p adjustment for multiple comparison). (*B*) HEK293 cells stably expressing SM-N100-GFP-V5 were conditioned in medium with or without 1 μM NB-598 for 16 h, then treated in conditioning medium with or without 20 μg/mL Chol/CD for 8 h. Graph shows densitometric representation of immunoblot of SM-N100-GFP-V5 cholesterol regulation. Data were normalized to cholesterol-mediated degradation in the vehicle condition, which was set to 100% (mean ± SEM; $n = 9$ independent experiments; **$P < 0.01$, two-sided paired *t* test versus vehicle). Gray open triangles denote raw data points.

We further tested this hypothesis by inhibiting squalene synthase (SQS), the enzyme preceding SM. Inhibiting SQS with TAK-475 eliminated the stabilization of SM-N100 by NB-598 (Fig. 4*E*, gray filled circle); however, supplementation of exogenous squalene restored stabilization by NB-598 (Fig. 4*E*, red filled triangle) to levels comparable to NB-598 treatment alone (Fig. 4*E*, black cross). These data clearly support the requirement of squalene for NB-598–mediated stabilization. Even in the absence of TAK-475, supplementation of exogeneous squalene resulted in additional

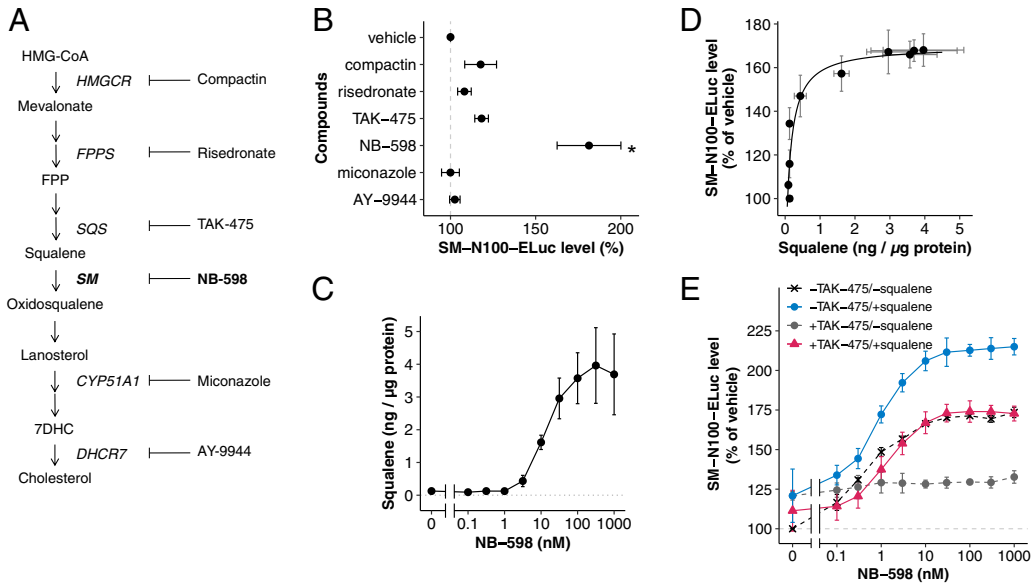

Fig. 4. Squalene accumulation mediates the stabilization of SM-N100 by NB-598. (*A*) Schematic representation of cholesterol biosynthesis enzymes and their inhibitors. (*B*) HEK293 cells stably expressing SM-N100-ELuc were treated with or without 1 μM inhibitor for 16 h, and expression levels were quantified by luciferase assay (black circles and error bars denote mean ± SD; $n = 3$ independent experiments). Multiple comparisons were performed using a Dunn Kruskal–Wallis test, and *P* values were adjusted based on the Benjamini–Hochberg correction ($n = 3$ independent experiments, $*P < 0.05$). (*C*) HEK293 cells stably expressing SM-N100-ELuc were treated with the indicated concentrations of NB-598 for 16 h, nonsaponifiable lipids were extracted, and squalene levels were analyzed using GC-MS (black circles and error bars denote mean ± SD; $n = 3$–4 independent experiments). See also *SI Appendix*, Fig. S2. (*D*) Correlation between squalene levels (from *C*) and SM-N100-ELuc levels (from Fig. 2*C*). Black circles and error bars indicate mean ± SD; black line indicates regression fit of a baseline-shifted Michaelis–Menten equation ($y = 59 + 111x/[x + 0.12]$). (*E*) HEK293 cells stably expressing SM-N100-ELuc were treated with the indicated concentrations of NB-598, with or without 10 μM TAK-475 and/or 300 μM squalene, as indicated for 16 h, and expression levels were quantified by luciferase assay (black circles and error bars denote mean ± SD; $n = 3$ independent experiments). Data were normalized to the vehicle condition (-TAK-475, -squalene, and 0 nM NB-598).

stabilization over NB-598 alone (Fig. 4*E*, blue filled circle). This also occurred for endogenous SM, likely due to the presence of NB-598 preventing metabolic consumption of the added squalene and, therefore, enhancing its stabilizing effects (*SI Appendix*, Fig. S4). Using TAK-475 cotreatment to separate squalene-mediated stabilization of the N100 domain from direct stabilization of the catalytic domain by NB-598, we also observed a larger contribution (>60%) of squalene-mediated stabilization for full-length SM-ELuc (*SI Appendix*, Fig. S5). Collectively, it is evident that NB-598–induced squalene accumulation mediates SM-N100 stabilization.

Squalene-Mediated Stabilization of SM Occurs at the ER Membrane. We have previously shown that SM-N100 localizes to the ER membrane (25). To examine if the squalene-mediated stabilization of SM-N100 also occurs at the ER membrane, we analyzed the distribution of SM-N100 using sucrose gradient subcellular fractionation in the absence or presence of accumulated squalene. Analysis of the fractions clearly showed that both SM-N100-ELuc and endogenous SM codistributed with calnexin, an ER membrane marker, but not with soluble proteins, plasma membranes, or Golgi markers (Fig. 5 and *SI Appendix*, Fig. S6). Although lysosomal membranes overlapped with ER membranes under the fractionation conditions, as reported previously (26, 27), immunocytochemical staining also supported the colocalization of SM-N100-ELuc with the ER marker (*SI Appendix*, Fig. S7). While SM has been reported to associate with lipid droplets (28), stabilization of SM occurred almost exclusively in the heavy, ER-enriched fractions and not in the lightest fraction, where lipid droplets are generally observed (29), arguing against the involvement of lipid droplets in this process. Inhibition of diacylglycerol acyltransferase, an enzyme required for lipid droplet biogenesis (30), also had no effect on the stabilization of SM-N100-ELuc by NB-598 (*SI Appendix*, Fig. S8), further confirming the dispensability of lipid droplets. Thus, we concluded that intracellular accumulation of squalene stabilizes SM at the ER membrane.

NB-598 and Squalene Stabilize SM-N100 by Blunting MARCH6 Interaction and Ubiquitination. MARCH6 is an ER-resident E3 ubiquitin ligase, which ubiquitinates SM (9) at the SM-N100 regulatory domain, targeting it for degradation (10, 11). Therefore, we hypothesized that squalene accumulation may stabilize SM-N100 by disrupting its MARCH6-mediated degradation.

Knockdown of *MARCH6* gene expression stabilized SM-N100 and endogenous SM but reduced the stabilizing effects of NB-598 treatment (Fig. 6*A*), suggesting that squalene stabilizes SM-N100 in a MARCH6-dependent manner. We next examined the interaction between SM-N100 and MARCH6 and found that while SM-N100 levels increased following NB-598 treatment (Fig. 6*B*, Input), there was no corresponding increase in MARCH6 interaction (Fig. 6*B*, Pellet). Accordingly, quantification showed that a smaller proportion of total SM-N100 was coimmunoprecipitated with MARCH6 (Fig. 6 *B*, *Lower Right*), indicating that squalene accumulation blunts their interaction.

In line with reduced MARCH6 interaction, exogenous squalene reduced the ubiquitination of SM-N100 (Fig. 6*C*). Collectively, these data showed that squalene and NB-598 regulate SM-N100 stability by interfering with its degradation by MARCH6.

Squalene Directly Binds to SM-N100 to Stabilize It. Next, we examined the specificity of the stabilizing effect of squalene by comparing it with its saturated analog, squalane. While squalene upregulated SM-N100, squalane did not have a significant effect (Fig. 7*B*) despite its similar biophysical behavior (31). The specificity of squalene over squalane led us to hypothesize that squalene directly binds to SM-N100 to modulate the stability of the N100 domain. To test this hypothesis, we synthesized a photoaffinity probe of

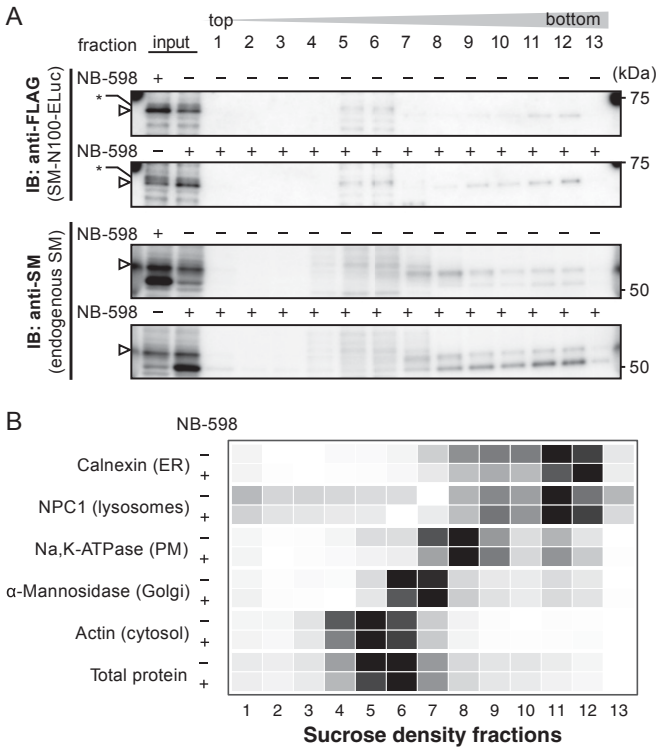

Fig. 5. Squalene-mediated stabilization occurs at the ER. (*A*) HEK293 cells stably expressing SM-N100-FLAG-ELuc were treated with or without 1 μM NB-598 for 16 h, and cell homogenates were fractionated by sucrose gradient ultracentrifugation. Fractions were collected and analyzed for the presence of SM-N100-FLAG-ELuc and endogenous SM by immunoblotting. Open arrowheads denote SM-N100-FLAG-ELuc or endogenous, full-length SM. Asterisk indicates a nonspecific band. Note that the fractions 5–6 showed higher background due to larger amount of total protein in the fractions. (*B*) The presence of the indicated organelle markers in cell fractions was quantified by immunoblotting or enzyme assays (see also *SI Appendix*, Fig. S6). Data are representative of $n = 2$ independent experiments with similar results.

squalene (SqBPY-153) and the corresponding saturated analog (SqBPY-150) as a negative-control probe (Fig. 7*A* and *SI Appendix*, *Supplementary Materials and Methods*). SqBPY-153 up-regulated SM-N100, whereas the saturated analog SqBPY-150 had no detectable effect, consistent with the specificity observed for squalene and squalane (Fig. 7*B*).

We next conducted photoaffinity-labeling experiments to examine if squalene and SqBPY-153 directly interact with SM-N100. SqBPY-153 labeled SM-N100 in an ultraviolet (UV)-dependent manner, while the inactive probe SqBPY-150 did not show significant labeling (Fig. 7*C*), again recapitulating the specificity observed for the up-regulatory effect (Fig. 7*B*). Furthermore, the SqBPY-153-mediated labeling was reduced by competition with squalene (Fig. 7*D*), clearly supporting the specific binding of squalene to SM-N100. We also found that oxygenated derivatives of squalene, which accumulate upon treatment with the oxidosqualene cyclase inhibitor BIBB-515, stabilized SM-N100 and competed with SqBPY-153 labeling (*SI Appendix*, Fig. S9). Together, these results demonstrated that squalene stabilizes the SM-N100 domain via direct binding.

Discussion

This work provides mechanistic insights into the regulation of human SM, an essential rate-limiting enzyme of cholesterol synthesis that is implicated in disease (32–35). The substrate of SM, squalene, is known to bind to the catalytic domain of SM. However, guided by chemical genetics (36, 37), we uncovered a mechanism by which squalene stabilizes SM via its noncatalytic N-terminal regulatory domain, SM-N100, providing evidence that an enzyme can be stabilized by its substrate binding to a site other than its active site.

Direct Binding of Squalene to SM. Squalene and its saturated analog squalane have been proposed to localize to the midplane of the lipid bilayer (31) and to affect membrane properties, thereby promoting lipid droplet budding from the ER membrane (38). Our data demonstrated that stabilization of SM-N100 was specifically observed with squalene and not with squalane (Fig. 7 *A* and *B*). In addition to squalene, we also noted that several oxygenated and more polar squalene analogs, including SqBPY-153 and oxidosqualene, stabilized SM-N100 and competed with the labeling (*SI Appendix*, Fig. S9). Although we cannot completely rule out contributions from other mechanisms, this selectivity argues against a membrane-mediated effect of squalene. Rather, our photoaffinity-labeling data suggests that the SM-N100 region creates a binding pocket that specifically recognizes squalene. A plausible physiological rationale for squalene-mediated stabilization of SM is that it would ensure sufficient SM levels to clear accumulated substrate (squalene).

During this study, we also observed a truncated form of endogenous SM (Figs. 2, 3, and 5 and *SI Appendix*, Figs. S2 and S4) that was strongly stabilized by NB-598, likely by its binding at the catalytic domain. Based on current evidence, we propose that this protein lacks the N100 degron of full-length SM, which is consistent with its strong stabilization by NB-598 (Fig. 2) and insensitivity to cholesterol treatment (Fig. 3). The origin of this truncated form of SM is currently under investigation.

Generalizing Findings to Other Lipids. The extent to which our findings can be generalized to other lipids that regulate SM is an important question. The degradation of SM is accelerated by cholesterol, requiring SM-N100 and MARCH6. Previously, we reported that SM senses membrane cholesterol (39), and that the SM-N100 amphipathic helix and reentrant loop undergo conformational changes with cholesterol excess (7, 8). Our current work clearly indicates that SM-N100 is more than just a cholesterol sensor (Fig. 8*C*). Indeed, unsaturated fatty acids and plasmalogens also alter SM protein stability (40, 41). Overall, SM has the ability to sense a variety of lipid species, and whether they all converge at a specific mechanism merits further investigation. Certainly, the blunting effect of squalene on cholesterol-mediated degradation of SM-N100 (Figs. 3*B* and 8*D*) is consistent with reduced MARCH6 interaction and ubiquitination (Fig. 6 *A*–*C*), given that this degradation is almost solely dependent on MARCH6 (10).

Implications for Other Studies. Although the structure of the catalytic domain of SM with NB-598 was recently published, the SM-N100 region has remained refractory to crystallization (12). Yet structural analyses should provide a clearer understanding of how SM-N100 senses squalene. Our finding that squalene stabilizes the SM-N100 domain may facilitate the purification and crystallization of this hydrophobic and disordered domain (42).

Squalene has long been used as an excipient for pharmaceutical applications, especially for the delivery of vaccines and drugs (43). However, as our work here indicates, it is more than an inert hydrocarbon and is being intently researched, including as an active ingredient in functional foods (44).

Much of the squalene exogenously added to cell culture is unlikely to be available to cells, as is often noted for sterols (45, 46). By contrast, inhibition of SM by NB-598 maximizes the intracellular accumulation of squalene, as shown by the ∼30-fold increase in total squalene abundance following NB-598 treatment (Fig. 4*C*). Although our results support the allosteric stabilization of SM by squalene at the ER membrane (Fig. 5), further studies

are required to directly address if such a feedforward regulation operates within physiological levels of endogenous squalene. Analysis of dose dependency does not adequately address this issue, as we must understand how squalene distributes within cells as well as local concentrations of squalene in the ER membrane, analogous to the distinct pools of cellular cholesterol (26).

Although the association of SM with lipid droplets has been reported, as has the accumulation of squalene in these compartments (28, 34, 38), we excluded a role for lipid droplet dynamics in squalene-mediated stabilization within our HEK293 cell models, which do not actively synthesize lipid droplets. In other cell types that produce a larger amount of lipid droplets, such as adipocytes, there may exist a cell type- or organ-specific role for squalene-lipid droplet dynamics in the regulation of SM proteostasis, offering an interesting area for further study.

Supporting the physiological relevance of its regulation by squalene, SM-N100 is responsive to small changes in squalene abundance: A 50% stabilization of SM-N100-ELuc occurred when squalene levels increased from ∼70 to ∼500 μg/g of total protein (Fig. 4*D*). There are several scenarios in which changes in squalene levels are likely to occur. First, given that SM is a rate-limiting enzyme in cholesterol biosynthesis (5), squalene levels will vary with the ebbs and flows of pathway flux. This includes the suppression of the pathway in response to LDL-cholesterol, which induces acute squalene accumulation (5). Under these circumstances, squalene-mediated stabilization of SM may increase the capacity of cells to rapidly resume the synthesis of cholesterol when its levels become limiting. Second, cholesterol synthesis is subject to diurnal variation, with threefold higher levels of lipoprotein-associated squalene during nighttime hours than during the day (47). Third, squalene concentrations are highly variable across human tissue types, ranging from ∼7 μg/g of dry weight in spleen to ∼75 μg/g in liver and ∼500 μg/g in skin, the latter two being notable sites of active cholesterol synthesis (48). Many of these concentrations are similar to those at which SM-N100 is most sensitive to squalene accumulation (Fig. 4*D*); therefore, squalene may assist in fine-tuning cell type- and tissue-specific rates of cholesterol synthesis according to supply and demand.

Given that molecular oxygen is required for the catalytic activity of SM, one situation in which squalene accumulation can

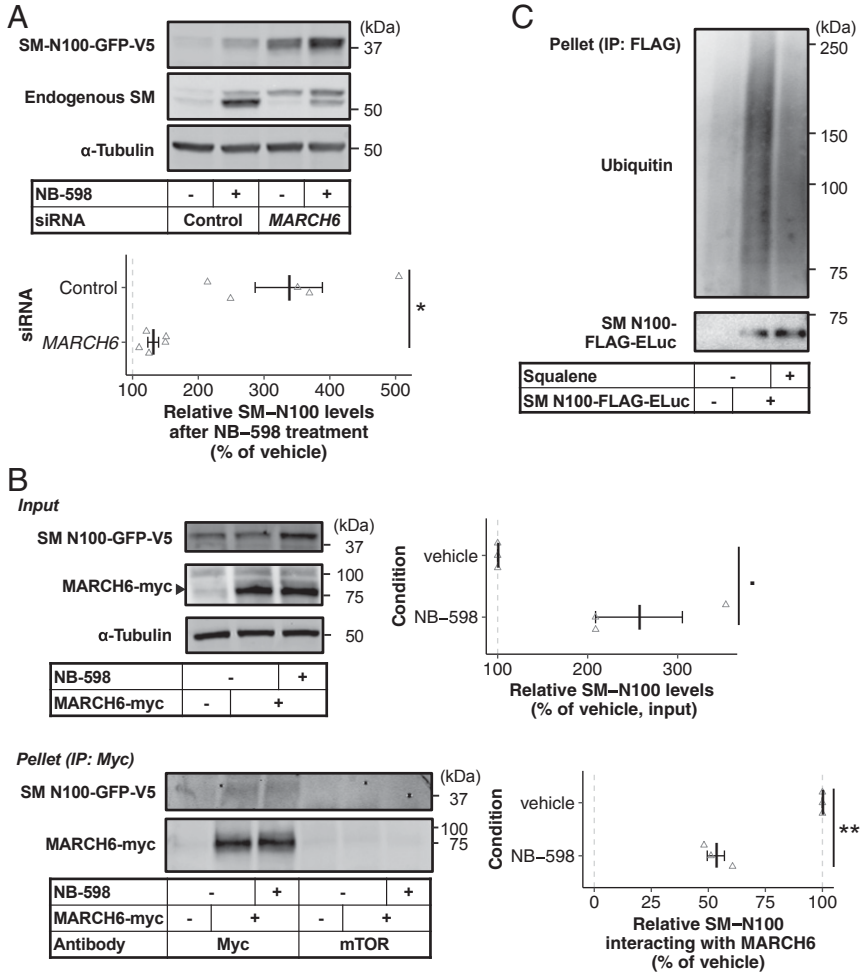

Fig. 6. Squalene stabilizes SM-N100 by blunting its interaction with MARCH6 and ubiquitination. (*A*) HEK293 cells stably expressing SM-N100-GFP-V5 were transfected with the indicated siRNA for 24 h and then treated with or without 1 μM NB-598 for 16 h. Graph shows densitometric representation of Western blot of SM-N100-GFP-V5 fold stabilization. Data were normalized to the vehicle condition, which was set to 100% (mean ± SEM; $n = 5$ independent experiments; $^{*}P < 0.05$, paired *t* test versus control siRNA). (*B*) HEK293 cells stably expressing SM-N100-GFP-V5 were transfected with MARCH6-myc for 24 h and treated with or without 1 μM NB-598 for 16 h. Equal protein amounts were immunoprecipitated using anti-myc antibody or anti-mTOR antibody as a specificity control, followed by immunoblotting. Graphs show densitometric representation of SM-N100-GFP-V5 levels in immunoprecipitation input, and relative interaction with MARCH6-myc. Data were normalized to the vehicle condition, which was set to 100% (mean ± SEM; $n = 3$ independent experiments; $^{\cdot}P < 0.1$, $^{**}P < 0.01$, paired *t* test versus vehicle). (*C*) HEK293 cells or HEK293 cells stably expressing SM-N100-FLAG-ELuc were treated with or without 300 μM squalene, in the presence of 10 μM CB-5083, 1 μM NB-598, and 10 μM TAK-475 for 6 h. Equal protein amounts were immunoprecipitated using anti-FLAG antibody, followed by immunoblotting.

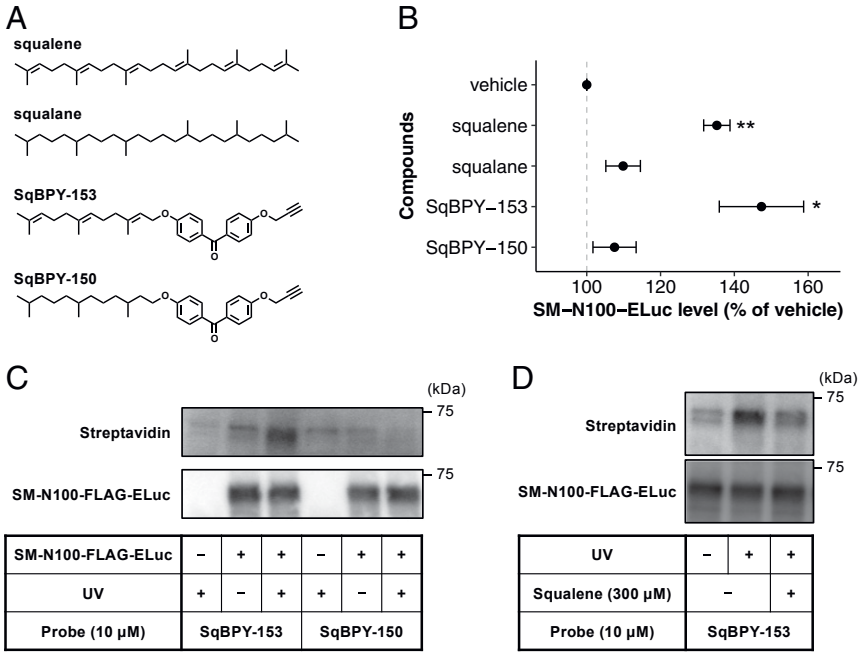

Fig. 7. Squalene is recognized by SM-N100 via direct binding. (*A*) Chemical structures of squalene, squalane, and corresponding photoaffinity probes. (*B*) HEK293 cells stably expressing SM-N100-ELuc were treated with 300 μM squalene, 300 μM squalane, 30 μM SqBPY-153, or 30 μM SqBPY-150 in the presence of 10 μM TAK-475 and 1 μM NB-598 for 16 h. SM-N100-ELuc expression levels were quantified by luciferase assay (mean ± SD, $n = 3$ independent experiments). Multiple comparisons were performed using a Dunn Kruskal–Wallis test, and *P* values are adjusted based on the Benjamini–Hochberg correction ($n = 3$ independent experiments, $*P < 0.05$, $**P < 0.01$). (*C*) Membrane fractions isolated from HEK293 cells or HEK293 cells stably expressing SM-N100-ELuc were treated with the indicated probes for 30 min at 4 °C and photoaffinity labeling was performed with 365-nm UV light for 3 min at 0 °C. Anti-FLAG–immunoprecipitated products were biotinylated by click chemistry followed by immunoblotting. Data are representative of $n = 2$ independent experiments. (*D*) Photoaffinity labeling was performed as described in *C* in the absence or presence of squalene. Data are representative of $n = 3$ independent experiments.

also occur is hypoxia (49). Under these circumstances, stabilization of SM may promote the clearance of accumulated squalene and its conversion to downstream cholesterol synthesis intermediates such as lanosterol, which potently suppresses the activity of the oxygen-intensive pathway (50). The fact that significant accumulation of squalene occurs only during prolonged hypoxia of greater than 6 h (49, 50) supports this sensitive buffering capacity of SM during periods of impaired catalytic activity. Consistent with a role for SM in adaptation to hypoxic stress, NB-598 treatment greatly increases the susceptibility of breast and colorectal cancer cells to hypoxia-induced cell death (51).

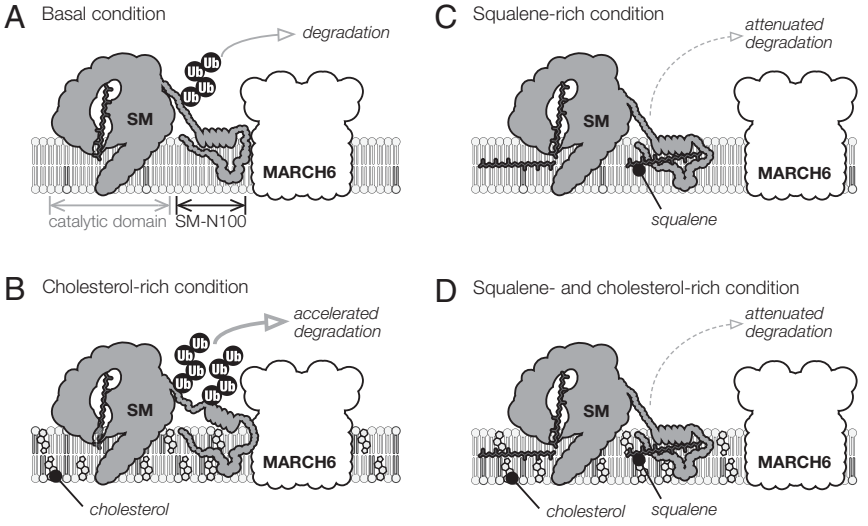

Fig. 8. Current model of SM regulation by squalene and cholesterol. (*A*) Under basal conditions, MARCH6 maintains steady-state levels of SM by ubiquitinating and targeting it for degradation. (*B*) During cholesterol excess, SM undergoes accelerated degradation in a MARCH6-dependent manner. (*C*) The SM-N100 regulatory domain senses squalene levels by directly binding squalene in the membrane, resulting in decreased interaction with MARCH6, decreased ubiquitination, and decreased degradation. (*D*) Squalene-rich conditions blunt the cholesterol-dependent degradation of SM-N100, perhaps by preventing cholesterol-induced conformational changes and recognition by MARCH6. This implies a feed-forward mechanism that prevents excessive accumulation of the SM substrate.

Recently, squalene accumulation has been noted in lymphoma and neuroendocrine cancer cells (34, 35). The metabolic vulnerability resulting from SM inhibition in neuroendocrine cancer cells is due to toxic squalene accumulation (34). Of note, a subset of neuroendocrine cancer cells lack sensitivity to SM inhibition as these cells could sequester toxic squalene. Contradicting this mechanism is the protective role of squalene accumulation in cholesterol auxotrophic lymphoma cancer cells (35). Cholesterol accumulation has a strong connection with prostate cancer, and studies have shown a link between the overexpression of *SQLE*, the gene encoding SM, and prostate cancer progression (52). Perhaps in these circumstances, prostate cancer cells have an increased capacity to direct squalene toward cholesterol production, in which case squalene-mediated stabilization of SM could be a contributing mechanism. However, the pathophysiological relevance of our findings in cancer cells requires further study.

In conclusion, we have found that squalene, the substrate of SM, stabilizes SM by binding to the N-terminal SM-N100 regulatory domain, thereby increasing the metabolic capacity at this rate-limiting enzyme. Such a local feedforward mechanism would help the cell to cope with sudden increases in metabolic flux and minimize excessive accumulation of squalene in the ER membrane, which could lead to altered membrane properties and the dysregulated production of lipid droplets (38). Thus, our finding has revealed another layer of regulatory mechanisms fine-tuning the cholesterol biosynthetic pathway and has shed light on the function of the SM-N100 regulatory domain. Furthermore, the ligandability of the SM-N100 domain demonstrated here may offer a renewed opportunity to control cholesterol biosynthesis by allosterically regulating SM, for which no active-site inhibitors have been approved for human use.

Materials and Methods

A more detailed, complete description of materials, cell culture, primers, and other methods is available in *SI Appendix, Materials and Methods*.

Chemical Screen. An expression vector for full-length SM fused to emerald luciferase (ELuc) was prepared by subcloning human SM sequence into the previously described blank ELuc-fusion vector, pCMV-AC-FLAG-ELuc (53). For more detail, see *SI Appendix, Materials and Methods*. A stable clone of HEK293 cells expressing pCMV-SM-ELuc was established and seeded in 96-well plates. After 48 h, the cells were treated with FDA-approved drugs at 1 μM or 10 μM for 16 h. Vehicle (0.1% dimethyl sulfoxide [DMSO]) and E1 inhibitor TAK-243 (10–0.01 μM) conditions were included as negative and positive controls. Expression levels of SM-ELuc were quantified by luciferase assay as follows: after removal of medium, 50 μL of luciferase substrate solution (1% Triton X-100, 250 μM D-luciferin, 1.5 mM ATP, 0.42 mM CoA, 30 mM, 100 mM 3-mercapto-1,2-propanediol, 100 mM tricine pH 7.8, 8 mM $Mg[OAc]_2$, and 0.2 mM ethylenediaminetetraacetic acid) was added, and luminescence was measured with an ARVO microplate reader (PerkinElmer) after 1 min. Luminescence data were plate-wisely normalized by sample median calculated from nonpositive-control samples, and converted into robust Z score, which is defined as effect size (each value–sample median) divided by median absolute deviation of the samples (54). Compounds that yielded a robust Z score of more than 5 for both concentrations and that gave reproducible effect in follow-up experiments were identified as hits. Dose–response analyses were similarly performed as described above.

Coimmunoprecipitation and Immunoblotting of SM-N100-GFP-V5. HEK-293 Flp-In T-REx cells stably expressing SM N100-GFP-V5 (HEK-SM-N100-GFP-V5) were generated previously (10). See *SI Appendix, Materials and Methods* for details.

Ubiquitination Assay. HEK293 cells stably expressing pCMV-SM-N100-FLAG-ELuc were seeded in six-well plates. After 48 h, the cells were treated with or without 300 μM squalene, in the presence of 10 μM CB-5083 (55), 1 μM NB-598, and 10 μM TAK-475 for 6 h. The cells were lysed in buffer supplemented with protease inhibitor mixture and *N*-ethylmaleimide (10 mM). SM-N100-FLAG-ELuc proteins were pulled down with anti-FLAG magnetic beads, immunoblotted for ubiquitin, and reprobed for FLAG. See *SI Appendix, Materials and Methods* for details.

Gas Chromatography–Mass Spectrometry Quantification of Squalene. Extraction of neutral, nonsaponifiable lipids was performed as previously described (5). Dried lipid extracts were silylated with *N,O*-bis(trimethylsilyl)trifluoroacetamide and analyzed by gas chromatography–mass spectrometry (GC-MS) in selective ion monitoring mode using a Thermo Trace gas chromatograph coupled with a Thermo DSQII mass spectrometer and Thermo Triplus autosampler (Thermo Fisher Scientific). The peak area of squalene was normalized to that of the 5α-cholestane internal standard, and quantification was performed using a squalene standard curve. See *SI Appendix, Materials and Methods* for details.

Subcellular Fractionation. Subcellular fractionation was performed based on previously reported protocols, with some modifications (26, 29). The indicated cell line was homogenized with a Balch homogenizer (isobiotec) in the presence of 15% (wt/vol) sucrose. After centrifugation (3,000 × *g* for 10 min at 4 °C), the postnuclear supernatant was fractionated on a discontinuous sucrose gradient (2%, 7.5%, 7.5%, 15%, 15%, 15%, 15%, 30%, 30%, 30%, 30%, 45%, 45%, each 1 mL, the input sample was loaded at the first two 15% sucrose layers). After ultracentrifugation at 125,000 × *g* for 1 h, 1-mL fractions were collected, and the presence of the indicated proteins or activity of the marker enzymes was analyzed. See *SI Appendix, Materials and Methods* for details.

Exogenous Supplementation of Squalene and Related Probes. Exogeneous supplementation of squalene was performed as described previously (56, 57), with minor modifications. Squalene and related probes were dissolved in a 1% solution of Tween 20 in DMSO to make 100× stock solutions. For cell treatment, the stock solutions were first prediluted in culture medium by 20-fold, and the prediluted solution (25 μL) was added to cell medium (100 μL) so that the final concentrations of Tween 20 and DMSO were 0.01% and 1%, respectively.

Chemical Synthesis of Squalene Probes. Synthesis and characterization of the photoaffinity probes SqBPY-153 and SqBPY-150 is described in *SI Appendix, Materials and Methods*.

Photoaffinity Labeling. Membrane preparation and photoaffinity labeling were performed as described previously (58), with some modifications. Briefly, membrane fractions isolated from HEK293 cells stably expressing pCMV-SM-N100-FLAG-ELuc were incubated on ice with the indicated probes (SqBPY-153 or SqBPY-150) and competitors for 30 min, and irradiated with ultraviolet (365 nm) for 3 min. The membrane was solubilized and biotin was conjugated to the alkyne via click chemistry. From the reaction mixture, FLAG-tagged SM-N100-ELuc was immunoprecipitated with anti-FLAG beads and separated by sodium dodecyl sulfate polyacrylamide gel electrophoresis. After transfer to a polyvinylidene difluoride membrane, the membrane was probed with streptavidin-horseradish peroxidase and reprobed with anti-FLAG antibody. See *SI Appendix, Materials and Methods* for details.

Data Availability Statement. All data discussed in the paper are included in this published article and *SI Appendix*. Screening data have been deposited to Mendeley Data (http://doi.org/10.17632/53dxyt4rnd.1).

ACKNOWLEDGMENTS. This work was supported in part by Grant-in-Aid for Young Scientists B from the Japan Society for the Promotion of Science (JSPS) (to K.O.) (JP17K15487); Grants-in-Aid for JSPS Research Fellow (to H.Y.) (JP18J14851); Grants-in-Aid for Scientific Research B (to Y.H.) (JP17H03996); and Australian Research Council Grant DP170101178 (to A.J.B.). We thank Dr. Martin Bucknall (University of New South Wales [UNSW] Bioanalytical Mass Spectrometry Facility) for training and technical assistance with GC-MS and the Faculty of Science at UNSW for their seed funding to support this work, the University of Tokyo Institute for Quantitative Biosciences Olympus Bioimaging Center for technical assistance with the FV3000 confocal microscope, and Dr. Ryuichiro Sato for encouraging our collaborative research.

1. M. S. Brown, A. Radhakrishnan, J. L. Goldstein, Retrospective on cholesterol homeostasis: The central role of Scap. *Annu. Rev. Biochem.* **87**, 783–807 (2018).
2. D. J. Chin *et al*., Sterols accelerate degradation of hamster 3-hydroxy-3-methylglutaryl coenzyme A reductase encoded by a constitutively expressed cDNA. *Mol. Cell. Biol.* **5**, 634–641 (1985).
3. G. Gil, J. R. Faust, D. J. Chin, J. L. Goldstein, M. S. Brown, Membrane-bound domain of HMG CoA reductase is required for sterol-enhanced degradation of the enzyme. *Cell* **41**, 249–258 (1985).
4. N. Sever, T. Yang, M. S. Brown, J. L. Goldstein, R. A. DeBose-Boyd, Accelerated degradation of HMG CoA reductase mediated by binding of insig-1 to its sterol-sensing domain. *Mol. Cell* **11**, 25–33 (2003).

5. S. Gill, J. Stevenson, I. Kristiana, A. J. Brown, Cholesterol-dependent degradation of squalene monooxygenase, a control point in cholesterol synthesis beyond HMG-CoA reductase. *Cell Metab.* **13**, 260–273 (2011).
6. A. V. Prabhu, W. Luu, L. J. Sharpe, A. J. Brown, Cholesterol-mediated degradation of 7-dehydrocholesterol reductase switches the balance from cholesterol to vitamin D synthesis. *J. Biol. Chem.* **291**, 8363–8373 (2016).
7. V. Howe, N. K. Chua, J. Stevenson, A. J. Brown, The regulatory domain of squalene monooxygenase contains a re-entrant loop and senses cholesterol via a conformational change. *J. Biol. Chem.* **290**, 27533–27544 (2015).
8. N. K. Chua, V. Howe, N. Jatana, L. Thukral, A. J. Brown, A conserved degron containing an amphipathic helix regulates the cholesterol-mediated turnover of human squalene monooxygenase, a rate-limiting enzyme in cholesterol synthesis. *J. Biol. Chem.* **292**, 19959–19973 (2017).
9. O. Foresti, A. Ruggiano, H. K. Hannibal-Bach, C. S. Ejsing, P. Carvalho, Sterol homeostasis requires regulated degradation of squalene monooxygenase by the ubiquitin ligase Doa10/Teb4. *eLife* **2**, e00953 (2013).
10. N. Zelcer *et al*., The E3 ubiquitin ligase MARCH6 degrades squalene monooxygenase and affects 3-hydroxy-3-methyl-glutaryl coenzyme A reductase and the cholesterol synthesis pathway. *Mol. Cell. Biol.* **34**, 1262–1270 (2014).
11. N. K. Chua, G. Hart-Smith, A. J. Brown, Non-canonical ubiquitination of the cholesterol-regulated degron of squalene monooxygenase. *J. Biol. Chem.* **294**, 8134–8147 (2019).
12. A. K. Padyana *et al*., Structure and inhibition mechanism of the catalytic domain of human squalene epoxidase. *Nat. Commun.* **10**, 97 (2019).
13. A. Nagumo, T. Kamei, J. Sakakibara, T. Ono, Purification and characterization of recombinant squalene epoxidase. *J. Lipid Res.* **36**, 1489–1497 (1995).
14. V. R. Viviani *et al*., Cloning and molecular characterization of the cDNA for the Brazilian larval click-beetle Pyrearinus termitilluminans luciferase. *Photochem. Photobiol.* **70**, 254–260 (1999).
15. Y. Nakajima *et al*., Enhanced beetle luciferase for high-resolution bioluminescence imaging. *PLoS One* **5**, e10011 (2010).
16. K. H. Choi, H. Basma, J. Singh, P.-W. Cheng, Activation of CMV promoter-controlled glycosyltransferase and beta -galactosidase glycogenes by butyrate, tricostatin A, and 5-aza-2′-deoxycytidine. *Glycoconj. J.* **22**, 63–69 (2005).
17. N. H. Pipalia *et al*., Histone deacetylase inhibitor treatment dramatically reduces cholesterol accumulation in Niemann-Pick type C1 mutant human fibroblasts. *Proc. Natl. Acad. Sci. U.S.A.* **108**, 5620–5625 (2011).
18. K. Subramanian, N. Rauniyar, M. Lavalleé-Adam, J. R. Yates, 3rd, W. E. Balch, Quantitative analysis of the proteome response to the histone deacetylase inhibitor (HDACi) vorinostat in niemann-pick type C1 disease. *Mol. Cell. Proteomics* **16**, 1938–1957 (2017).
19. M. Horie *et al*., NB-598: A potent competitive inhibitor of squalene epoxidase. *J. Biol. Chem.* **265**, 18075–18078 (1990).
20. Y. Iwasawa, M. Horie, Mammalian squalene epoxidase inhibitors and structure-activity relationships. *Drugs Future* **18**, 911–918 (1993).
21. D. J. MacEwan, G. Milligan, Inverse agonist-induced up-regulation of the human beta2-adrenoceptor in transfected neuroblastoma X glioma hybrid cells. *Mol. Pharmacol.* **50**, 1479–1486 (1996).
22. P. A. Stevens, N. Bevan, S. Rees, G. Milligan, Resolution of inverse agonist-induced upregulation from constitutive activity of mutants of the alpha(1b)-adrenoceptor. *Mol. Pharmacol.* **58**, 438–448 (2000).
23. D. Ramsay, N. Bevan, S. Rees, G. Milligan, Detection of receptor ligands by monitoring selective stabilization of a Renilla luciferase-tagged, constitutively active mutant, G-protein-coupled receptor. *Br. J. Pharmacol.* **133**, 315–323 (2001).
24. A. I. Alexandrov, M. Mileni, E. Y. T. Chien, M. A. Hanson, R. C. Stevens, Microscale fluorescent thermal stability assay for membrane proteins. *Structure* **16**, 351–359 (2008).
25. N. K. Chua, N. A. Scott, A. J. Brown, Valosin-containing protein mediates the ERAD of squalene monooxygenase and its cholesterol-responsive degron. *Biochem. J.* **476**, 2545–2560 (2019).
26. A. Radhakrishnan, J. L. Goldstein, J. G. McDonald, M. S. Brown, Switch-like control of SREBP-2 transport triggered by small changes in ER cholesterol: A delicate balance. *Cell Metab.* **8**, 512–521 (2008).
27. L. Abi-Mosleh, R. E. Infante, A. Radhakrishnan, J. L. Goldstein, M. S. Brown, Cyclodextrin overcomes deficient lysosome-to-endoplasmic reticulum transport of cholesterol in Niemann-Pick type C cells. *Proc. Natl. Acad. Sci. U.S.A.* **106**, 19316–19321 (2009).
28. R. Leber *et al*., Dual localization of squalene epoxidase, Erg1p, in yeast reflects a relationship between the endoplasmic reticulum and lipid particles. *Mol. Biol. Cell* **9**, 375–386 (1998).
29. Y. Fujimoto *et al*., Identification of major proteins in the lipid droplet-enriched fraction isolated from the human hepatocyte cell line HuH7. *Biochim. Biophys. Acta* **1644**, 47–59 (2004).
30. C. A. Harris *et al*., DGAT enzymes are required for triacylglycerol synthesis and lipid droplets in adipocytes. *J. Lipid Res.* **52**, 657–667 (2011).
31. T. Hauss, S. Dante, N. A. Dencher, T. H. Haines, Squalane is in the midplane of the lipid bilayer: Implications for its function as a proton permeability barrier. *Biochim. Biophys. Acta* **1556**, 149–154 (2002).
32. A. Chugh, A. Ray, J. B. Gupta, Squalene epoxidase as hypocholesterolemic drug target revisited. *Prog. Lipid Res.* **42**, 37–50 (2003).
33. G. Cirmena *et al*., Squalene epoxidase as a promising metabolic target in cancer treatment. *Cancer Lett.* **425**, 13–20 (2018).
34. C. E. Mahoney *et al*., A chemical biology screen identifies a vulnerability of neuroendocrine cancer cells to SQLE inhibition. *Nat. Commun.* **10**, 96 (2019).
35. J. Garcia-Bermudez *et al*., Squalene accumulation in cholesterol auxotrophic lymphomas prevents oxidative cell death. *Nature* **567**, 118–122 (2019).
36. S. L. Schreiber, Chemical genetics resulting from a passion for synthetic organic chemistry. *Bioorg. Med. Chem.* **6**, 1127–1152 (1998).
37. M. Côté *et al*., Small molecule inhibitors reveal Niemann-Pick C1 is essential for Ebola virus infection. *Nature* **477**, 344–348 (2011).
38. K. Ben M'barek *et al*., ER membrane phospholipids and surface tension control cellular lipid droplet formation. *Dev. Cell* **41**, 591–604.e7 (2017).
39. I. Kristiana *et al*., Cholesterol through the looking glass: Ability of its enantiomer also to elicit homeostatic responses. *J. Biol. Chem.* **287**, 33897–33904 (2012).
40. J. Stevenson, W. Luu, I. Kristiana, A. J. Brown, Squalene mono-oxygenase, a key enzyme in cholesterol synthesis, is stabilized by unsaturated fatty acids. *Biochem. J.* **461**, 435–442 (2014).
41. M. Honsho, Y. Abe, Y. Fujiki, Dysregulation of plasmalogen homeostasis impairs cholesterol biosynthesis. *J. Biol. Chem.* **290**, 28822–28833 (2015).
42. M. Vedadi *et al*., Chemical screening methods to identify ligands that promote protein stability, protein crystallization, and structure determination. *Proc. Natl. Acad. Sci. U.S.A.* **103**, 15835–15840 (2006).
43. L. H. Reddy, P. Couvreur, Squalene: A natural triterpene for use in disease management and therapy. *Adv. Drug Deliv. Rev.* **61**, 1412–1426 (2009).
44. H. Narayan Bhilwade *et al*., The adjuvant effect of squalene, an active ingredient of functional foods, on doxorubicin-treated allograft mice. *Nutr. Cancer* **71**, 1153–1164 (2019).
45. B. A. Janowski *et al*., Structural requirements of ligands for the oxysterol liver X receptors LXRalpha and LXRbeta. *Proc. Natl. Acad. Sci. U.S.A.* **96**, 266–271 (1999).
46. S. Nachtergaele *et al*., Oxysterols are allosteric activators of the oncoprotein Smoothened. *Nat. Chem. Biol.* **8**, 211–220 (2012).
47. T. A. Miettinen, Diurnal variation of cholesterol precursors squalene and methyl sterols in human plasma lipoproteins. *J. Lipid Res.* **23**, 466–473 (1982).
48. G. C. Liu, E. H. Ahrens, Jr, P. H. Schreibman, J. R. Crouse, Measurement of squalene in human tissues and plasma: Validation and application. *J. Lipid Res.* **17**, 38–45 (1976).
49. P. Kucharzewska, H. C. Christianson, M. Belting, Global profiling of metabolic adaptation to hypoxic stress in human glioblastoma cells. *PLoS One* **10**, e0116740 (2015).
50. A. D. Nguyen, J. G. McDonald, R. K. Bruick, R. A. DeBose-Boyd, Hypoxia stimulates degradation of 3-hydroxy-3-methylglutaryl-coenzyme A reductase through accumulation of lanosterol and hypoxia-inducible factor-mediated induction of insigs. *J. Biol. Chem.* **282**, 27436–27446 (2007).
51. S. Haider *et al*., Genomic alterations underlie a pan-cancer metabolic shift associated with tumour hypoxia. *Genome Biol.* **17**, 140 (2016).
52. K. H. Stopsack *et al*., Cholesterol metabolism and prostate cancer lethality. *Cancer Res.* **76**, 4785–4790 (2016).
53. S. Nanjyo *et al*., Structure-activity relationship study of estrogen receptor downregulators with a diphenylmethane skeleton. *Bioorg. Med. Chem.* **27**, 1952–1961 (2019).
54. I. Coma, J. Herranz, J. Martin, Statistics and decision making in high-throughput screening. *Methods Mol. Biol.* **565**, 69–106 (2009).
55. E. Y. Huang *et al*., A VCP inhibitor substrate trapping approach (VISTA) enables proteomic profiling of endogenous ERAD substrates. *Mol. Biol. Cell* **29**, 1021–1030 (2018).
56. T. Ikekawa *et al*., [Studies on antitumor activity of squalene and its related compounds]. *Yakugaku Zasshi* **106**, 578–582 (1986).
57. F. R. Santori *et al*., Identification of natural RORγ ligands that regulate the development of lymphoid cells. *Cell Metab.* **21**, 286–298 (2015).
58. K. Ohgane, F. Karaki, K. Dodo, Y. Hashimoto, Discovery of oxysterol-derived pharmacological chaperones for NPC1: Implication for the existence of second sterol-binding site. *Chem. Biol.* **20**, 391–402 (2013).